



Contents lists available at ScienceDirect

Journal of King Saud University – Science

journal homepage: www.sciencedirect.com



Original article

Photocatalytic degradation and anti-cancer activity of biologically synthesized Ag NPs for inhibit the MCF-7 breast cancer cells

Govindan Nadar Rajivgandhi^{a,b}, Govindan Ramachandran^b, Moorthy Rajesh Kannan^c, Arockiam Antony Joseph Velanganni^c, Muhammad Zubair Siddiqi^d, Naiyf S. Alharbi^e, Shine Kadaikunnan^e, Wen-Jun Li^{a,f,*}

^a State Key Laboratory of Biocontrol, Guangdong Provincial Key Laboratory of Plant Resources and Southern Marine Science and Engineering Guangdong Laboratory (Zhuhai), School of Life Sciences, Sun Yat-Sen University, Guangzhou 510275, PR China

^b Department of Marine Science, Bharathidasan University, Tiruchirappalli 620024, Tamil Nadu 620024, India

^c Department of Biochemistry, Bharathidasan University, Tiruchirappalli 620024, Tamil Nadu, India

^d Department of Biotechnology, Hankyong National University, 327 Jungang Road, Gyeonggi-do 17579, South Korea

^e Department of Botany and Microbiology, College of Science, King Saud University, Riyadh 11451, Saudi Arabia

^f State Key Laboratory of Desert and Oasis Ecology, Xinjiang Institute of Ecology and Geography, Chinese Academy of Sciences, Urumqi 830011, PR China

ARTICLE INFO

Article history:

Received 25 September 2021

Revised 12 November 2021

Accepted 16 November 2021

Available online 22 November 2021

Keywords:

Phytochemical screening

Silver nanoparticle

DPPH scavenging activity

Anti-cancer activity

And photocatalysis

ABSTRACT

The current study was aimed to detect the enhanced anti-cancer and photo catalytic dyes degradation effect of marine mangrove plant *Rhizophora mucronata* mediated Ag NPs. The UV-spectrometer data of surface peak renounces for synthesized Ag NPs indicated at 415 nm and all the functional groups and morphological structures were shown in XRD, SEM. In addition, the clear spherical morphology of SEM image was indicated the original crystalline and mono dispersive nature of silver nanoparticle structure. Further, the anti-oxidant activity result was clearly stated that the Ag NPs has enhanced biological properties and it shown with dose dependent anti-cancer activity against MCF-7 lung cancer cells. All the fluorescence microscopic images suggested that the Ag NPs was enhanced the apoptosis in MCF-7 cells. Photocatalytic degradation effect of synthesized silver nanoparticles effectively removed the dye.

© 2021 The Author(s). Published by Elsevier B.V. on behalf of King Saud University. This is an open access article under the CC BY-NC-ND license (<http://creativecommons.org/licenses/by-nc-nd/4.0/>).

1. Introduction

Recent years, the synthesis of nanoparticles has addressed increased attention for biomedical field based on the properties of chemical, physical and biological with clean, reliable and biocompatible nature (Gomathi et al., 2020). Especially, silver nanoparticle is frequently synthesized, efficient characters with increased bioactivity nature, which is used very high in the biomedical application (Ramar et al., 2015). The Ag NPs are often

supported to different industrial applications including cosmetics, food, environment, catalyst and biopharmaceutical. Most researchers concentrated to synthesis only Ag NPs owes to its advantages and versatile medicinal properties including microbes, virus, mosquito and wound healing (Almalki and Khalifa, 2020). Compared with other nanoparticles, the Ag is the most reported nanoparticles with excellent biological properties (Uzma et al., 2020; Titkov et al., 2017).

The researchers are employed many routes for synthesis of Ag NPs, they are hydrothermal decomposition, electrochemical reduction, microwave assisted, microbes and green mediated procedures (Dinparvar et al., 2020). Currently, more utilization of energy by other methods is not efficient completely due to the high level toxicity production. Also, it has delivered high operation cost compared with biological route of green synthesis (Ghosal et al., 2020). Green synthesized Ag NPs using plant extract has opened a new route for delivering alternative method for produce potential nanoparticle (Jiang et al., 2014; Mortazavi-Derazkola et al., 2020). In green synthesis, the different biological resources utilized methods are used to synthesize the nanoparticles such as

* Corresponding authors at: State Key Laboratory of Biocontrol, Guangdong Provincial Key Laboratory of Plant Resources and Southern Marine Science and Engineering Guangdong Laboratory (Zhuhai), School of Life Sciences, Sun Yat-Sen University, Guangzhou 510275, PR China (W.-J. Li).

E-mail address: liwenjun3@mail.sysu.edu.cn (W.-J. Li).

Peer review under responsibility of King Saud University.



Production and hosting by Elsevier

microbes, algae, plant and some other sources. Among these biological sources, plant mediated Ag NPs are the most reliable and promising method, it has environmental friendly nature having potential bioactivities (Al-kawmani et al., 2020). The effect of plant mediated Ag NPs has increased the anti-oxidant and variety of cancer cells. In particular, many researchers are suggested previously that the silver nanoparticles very effective for cancer cells and also recommended to development of new drugs against various cancer cells (Solairaj et al., 2017). Silver nanoparticle is very toxic nature to cancer cells, and interior proliferation efficiency due to the some liability of signaling cascades for the development of pathogenesis of cancer (Khorrami et al., 2019). In plant mediated Ag NPs synthesis, reducing agent of purified extract was used frequently and stabilized the synthesized material (Uzma et al., 2020). All the plant parts of leaves, stems, roots and other parts are used for synthesis of nanoparticles. In plant mediated synthesis, the Ag ions were reduced and formed as Ag NPs by the capping of plant extract chemical constituents by the process of catalysis (Majeed et al., 2019). Taken together, the present study focused on flavonoid, polyphenols, phenolic acids, alkaloids, terpenoids rich marine mangrove plant of *Rhizophora mucronata* was performed to synthesis silver nanoparticles for various applications.

2. Materials and methods

2.1. Preparation of plant extract

Well grinded plant leaves were taken and mixed into the sterile 100 millipore water and continually heated at 80 °C for 1 h. After, the process was cool and the fine liquid format of the sample was filtered using whatman No. 5 filter paper. Then, the sample was mixed in methanol of soxhlet experiment procedure and run 3 h with room temperature. Then, methanol was removed gradually and collected filtrate was maintained under reduced pressure at 45 °C for 1 day with the help of rotary evaporator. Finally the color changes of the sample turn to dark green was noted and used for synthesis of nanoparticle process.

2.2. GC–MS analysis

The active compounds present in the *Rhizophora mucronata* extract was spectroscopically analyzed by GC–MS (GKR international, GmbH, and Darmstadt, Germany). In GC–MS, varian chromatograph CP-3800 GC/MS/MS-200 equipped with split-splitless injector, 20 m × 0.25 mm, I.D of 0.25 μm thickness of film was used. In addition, the non-polar column was used for fractionation. The following conditions were set in the analyzed GC–MS: The detector temperature – 260–280 °C; injector temperature – 250 °C; carrier gas He (1 mL/min), split ratio – 30, injection volume 0.2 μL, Mass range m/z = 20–450. The oven temperature was maintained at 120 °C for 2 min; programmed to 280 °C at rate of 5°C/min. The consent temperature of 280 °C for 15 min was used. The film was coated with non-polar column and also the oven temperature was maintained at 30–380 °C time intervals. Additionally, 70 eV ionization voltage of ultra-helium was acted as a gas carrier with flow rate of 1.0 mL/min (Ramachandran et al., 2020).

2.3. Measurement of phenol and flavonoid properties

The Folin–Ciocalteu's mediated phenolic properties in the *Rhizophora mucronata* extract was measured by UV-spectrometer analysis using Gallic acid as standard (Rajivgandhi et al., 2020). The 0.5 mL of *Rhizophora mucronata* extract was diluted by Folin–Ciocalteu's solution with required concentration and followed by 2ML of Na₂CO₃. The diluted solution was shaken vigorously for

5 min and maintained in dark room at least 30 min. Finally, read on spectrophotometer at 510 nm. Consecutively, the final concentration (10–100 μg/mL) of gallic acid was used as a positive control with same procedure. The result was interpreted with 1 μg of and it equal to 1 g of the powder. Further, the amount of flavonoid content in the *Rhizophora mucronata* extract was estimated by colorimetric assay using rutin as a standard. The short method of flavonoid detection was followed by Rajivgandhi et al. (2020), and 150 μL sodium nitrate and 400 μL of extract solution taken together with with 150 μL of sodium nitrate was taken initially in a fresh tube. 10% w/v aluminium chloride and KI also added into the side wall of the tube. Then the result was followed by incubated at room temperature in dark condition for 30 min as same as for control also. After incubation, both the samples were measured at 540 nm O.D. 1 mg of flavonoid result was considered when it compared with 1 μg gallic acid.

2.4. Anti-oxidant activity

Phosphor molybdenum method was performed to detect their anti-oxidant activity (Ramesh et al., 2018). Initially, sodium phosphate, ammonium molybdate and sulphuric acid were mixed thoroughly at 97 °C for 45 min in water bath. 10 μL of purified extract was diluted into the 1 mL of prepared solution and allowed to stands for 30 min. After incubation, the mixed solution produced anti-oxidant rate was calculated by biophotometer (Sigma, India) at the wave length of 590 nm O.D. Finally, the anti-oxidant activity of tested material was compared with ascorbic acid control result for proper interpretation and the anti-oxidant activity was considered to microgram of ascorbic acid as equivalents to purified fraction.

2.5. DPPH free radical scavenging assay

The DPPH radical scavenging activity of purified *Rhizophora mucronata* extract was carried out according to the previous method of Rajivgandhi et al. (Rajivgandhi et al., 2020). Various concentration 50, 100, 150, 200, 250, 300, 350 of purified plant extract was aliquot and 3 μL of butylated hydroxyl toluene, which acted as a standard control were taken together in the 200 μL DPPH mixed ethanol tube. The treated and untreated sample tubes were shaken rapidly and maintained at dark condition in room for 30 min. The solution of ethanol containing tube served as a blank. After incubation, the anti-oxidant activity of sample tubes was measured using spectrophotometer. Finally, the test sample result was compared with standard control and calculated the differentiation,

$$DPPH\ scavenged(\%) = [(Control\ OD - Test\ OD)/(Control\ OD) \times 100]$$

2.6. Synthesis and characterization of Ag NPs

Aqueous solution of 1: 10 ratios of plant material (1 mL) and Ag NO₃ (10 mL) were used to silver nanoparticle synthesis in 50 mL with the help of reported article (Saravanakumar et al., 2019; Kumar et al., 2019). The sample was put it in water bath with one hour and the pH was adjusted properly 1 N H₃PO₄ between the gaps. After one hour, the changed yellow to orange or brown color and it suggested the mixture of the materials were silver nanoparticle. Consecutively, the synthesized Ag NPs was first checked by UV–vis spectroscopy. Synthesized Ag NPs and their electrical vibration connectivity was detected by XRD at the wave ranges of 10°–80°. After, surface morphology was scanned by scanning electron microscope

2.7. Anti-cancer activity analysis

2.7.1. Viability of MCF-7 cells using biosynthesized Ag NPs

The MCF breast cancer cells viability of biosynthesized Ag NPs was monitored after using dimethylthiazol-diphenyltetrazolium bromide (MTT) by UV-spectrophotometer (Venugopal et al., 2017). Firstly, the aliquot DMEM medium was made for complete medium with necessary procedure and then required quantity of the medium was filled in 96-well plate. In addition, $\sim 2 \times 10^4$ of breast cancer cells were diluted and maintained in presence of 5% CO₂ condition with incubation. Humidity range of 95% used exactly. Consecutively, 5–100 $\mu\text{g}/\text{mL}$ concentration of treated silver nanoparticle with increasing order of the 96-wells containing sample before incubation. Whereas, the DMEM alone plus MCF-7 cells of the well-used as positive control and MCF-7 cells plus negative control of DMSO used. MTT solution was added in all wells and packed by aluminum foil. Final formazan crystal production of process happened in inside of the wells were watched. Based on the observation, the interactions between Ag NPs and MCF-7 breast cancer cells were confirmed using the calculation of formed color intensity by 540 nm O.D of UV-spectrometer. The result was done and taken in triplicated result, and the viability of MCF-7 cells measured by bellowed calculation,

$$\%IC_{50} = [\text{Control O.D}_1 - \text{Test O.D}] \times 100.$$

For calculation, untreated wells were not affected due to absence of silver nanoparticle, so, the control result was used with 100%, and the treated results were compared to control result for detection of viability in the 96-well plate. Finally, the 50% viability of the well containing concentration was fixed as IC₅₀ concentration.

2.7.2. Analysis of structural changes

The morphological alteration in the Ag NPs treated 6-well plate of MCF-7 cells were morphologically observed by phase contrast microscope using previous reported work of Naveen Kumar et al., 2018; Khataee and Kasiri, 2010). Firstly, the overnight MCF-7 cells were taken in 6-well plate with DMEM medium, and followed by treatment of IC₅₀ concentration of Ag NPs in same well. Then incubated with required temperature with inside cover slip. Then, the plate was taken form incubator and fixed by using 1% formaldehyde on the cover slip containing sample for 30 min. Lastly, the untreated and treated wells of the MCF-7 cells on the cover slip was taken and checked the changes of both the cover slip containing morphology was viewed microscopic analysis

2.7.3. Live/dead differentiation

The fluorescence observation morphology in the presence of IC₅₀ concentration of Ag NPs against MCF-7 breast cancer cells was viewed by fluorescent microscope (Ramar et al., 2015). The six well plates were filled by need DMEM medium and MCF-7 breast cancer cells and soaked on a cover slip properly. Then, cover slip of treated cancer cells and also as same as procedure without addition of biosynthesized Ag NPs for control well of cover slip was used. Both the cover slips of the six well plates were put in room atmosphere. After half day, both the cover slips were taken from the 6-well plate and unattached cells were rinsed clearly by using 1x PBS. Then, the attached cells of both the cover slips were allowed to dilute by 10 $\mu\text{g}/\text{mL}$ AO/EB combination. Lastly, the samples of the cover slips were directly seen in the fluorescence microscope using AO/EB staining for detection of morphological modification.

2.8. Photocatalytic activity

The efficiency of degradation of Rhodamine B (Rho B) and Crystal violet (CV) by Ag NPs was evaluated using the method described by Khataee and Kasiri (S.K., et al., 2017). 1 mg/L of Rho B and CV solution was prepared using deionized water. At the same different concentration of Ag NPs (5, 10 and 15 mg/L) was added into the conical flask containing different concentration of Rho B and CV solutions. This experimental setup was maintained by exposing continuous white light fewer than 160 rpm for 3hrs. The aliquots of 5 mL from experimental setup was collected every 30mins to analysis the concentrations of Rho B and CV. The concentration of Rho B was analyzed using UV-visible spectrophotometry. The lambda max values of Rho B and CV was determined as 553 and 585 nm respectively. The percentage of dye degradation was calculated by following formula (1)

$$\% \text{degradation} = \frac{(C_0 - C)}{C_0} * 100 \quad (1)$$

3. Result and discussion

3.1. Identification of chemical composition

The exhibited peaks of the GC-MS were shown with 35 different peaks, and all the peaks were exhibited with different pyto-compounds. All the compounds were clearly confirmed after interpretation of Sun Yat-Sen University Wiley library, and the compounds have potential biological properties. Among the various peaks, the alkaloids, flavonoids and phenolic compounds were screened separately and followed by bioactive compounds screened separately. Compared with previous reports, the phenol and flavonoid rich compounds have significant anti-oxidant activity (Majeed et al., 2019; Yang et al., 2020). This statement was good agreed by recent studies of Gomathi et al. (Gomathi et al., 2020); pyto-compounds have more antioxidant activities. Previously, *Rhizophora mucronata* extract has rich phenol and flavonoid contents and it possesses excellent anti-oxidant activity with significant biological properties (Rajivgandhi et al., 2020; Rajivgandhi et al., 2020). They anti-cancer ability of the compound names are 7,9-Di-tert-butyl-1-oxaspiro(4,5)deca-6,9-diene-2,8-dione, Pyrrolo[1,2-a]pyrazine-1,4-dione, hexahydro-3-(2-methylpr, 1-Octadecene, Chirysin 1, 2, 3, Phthalate and Phenol, 2,4-bis(1,1-dimethylethyl). The retention times, occupation area and occupation percentages were shown with 30,42, 28.34, 20, 15, 15, 67, 12, 32 and 24, 78 and 40,6758, 32,4765, 60,7098, 28, 6754, 24, 5674, and 23, 45,342 respectively (Fig. 1). Further, the identified compounds might be potential anti-cancer compounds compared with other sources unfavorable conditions of nutrients, and salt concentration, and other contents.

3.2. Measurement of phenol and flavonoid properties

After careful comparison with positive controls of gallic acid (R₂ = 0.9661) for phenolic and rutin (R₂ = 0.9690) for flavonoid, the linearity calibration curves of phenolic and flavonoid contents were very high at 10–100 $\mu\text{g}/\text{mL}$ (Fig. 2a, b). It was comparatively very higher than other plants reported previously. Therefore, when the results were compared with sugar and protein levels, the phenol and flavonoid properties were very high. The agreed result was reported by Yang et al. (Aji Jovitha and Deivasigamani, 2020) and the marine mangrove plant *Rhizophora mucronata* has more phenolic and flavonoid derivatives compared with other terrestrial plants. It may be influenced by unpredictable mangrove environment including high temperature, pH, NaCl, different ratio of car-

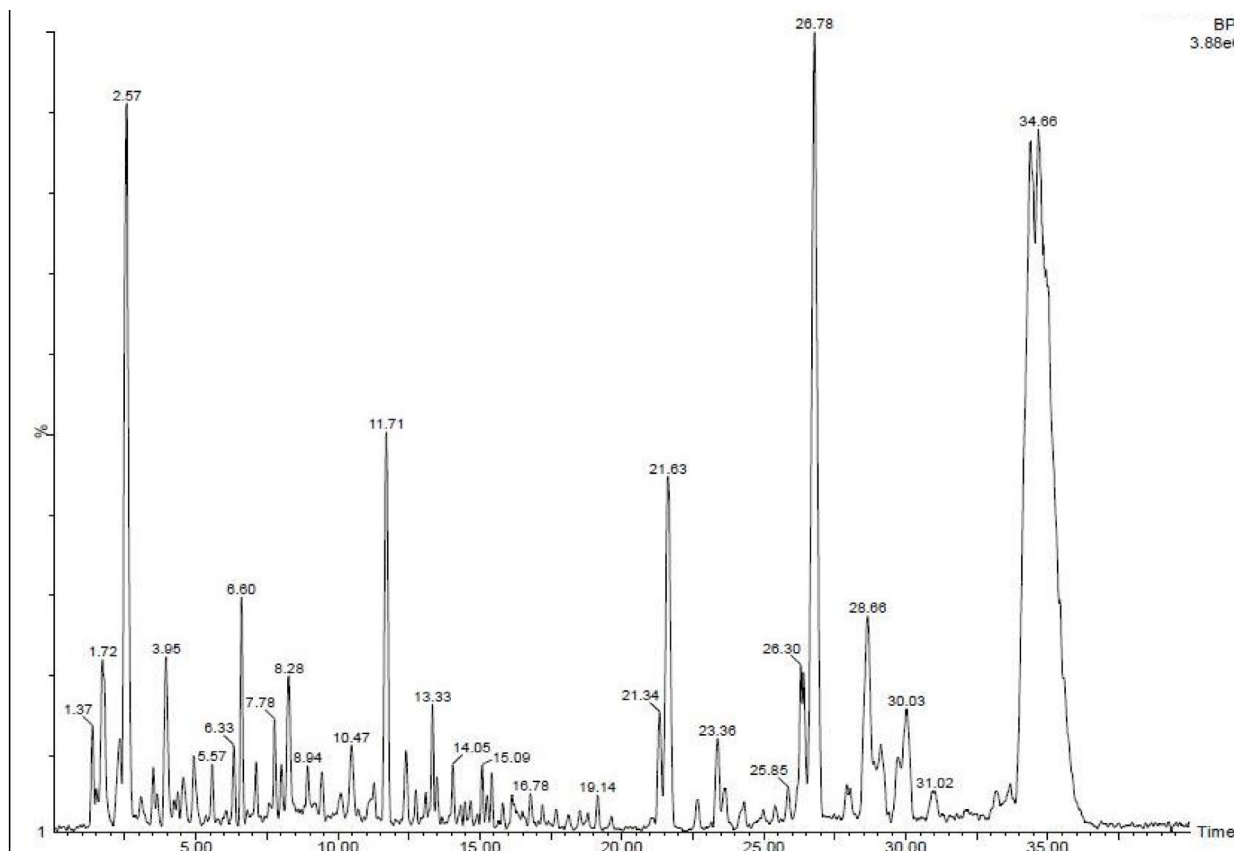


Fig. 1. GC-MS analysis reports of available chemical compounds in the *Rhizophora mucronata* extract.

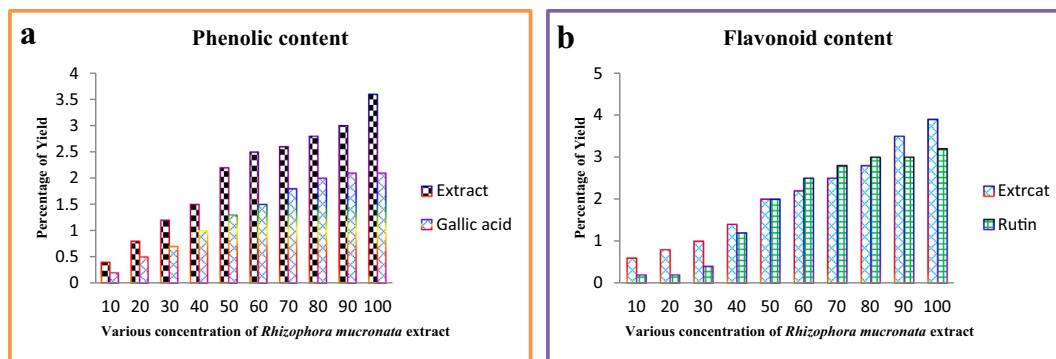


Fig. 2. Measurement of phenolic and flavonoid contents of the *Rhizophora mucronata* extract.

bon-nitrogen sources and other stress conditions. This extreme condition plant has the ability to produce excellent bioactivity compounds, particularly anti-cancer compounds (Khorrami et al., 2019). So, the *Rhizophora mucronata* mediated synthesis is an important source for improved bioactivity of nanoparticles synthesis.

3.3. Measurement of anti-oxidant activity

The increasing level of anti-oxidant activity of plant extract was suggested that the plant possess high phenolic and flavonoid content. As well as, the increased content of phenolic and flavonoid derivatives led to stimulate the increased anti-oxidant activity (Majeed et al., 2019; Ramachandran et al., 2020). Based on this statement, our result was indicated that the *Rhizophora mucronata*

extract has increased anti-oxidant activity than synthesized Ag NPs. In addition, the positive control of ascorbic acid was also showed increased anti-oxidant activity than Ag NPs, and closely related value to *Rhizophora mucronata* extract. The anti-oxidant activities of *Rhizophora mucronata* extract, Ag NPs and ascorbic acid were exhibited the O.D value of 0.877, 0.490, 0.896 at 150 µg/mL respectively. The total anti-oxidant activity result was concluded that the Ag NPs has decreased activity than extract and control at increased concentration, as well as no significant differences between extract and control was recorded.

The variations of performed samples result was presented in Fig. 3a. Interestingly, the increased free radical activity of DPPH assay result was shown to Ag NPs compared with extract and positive control of ascorbic acid. At increasing concentration, the Ag NPs was exhibited excellent free radical scavenging activity with

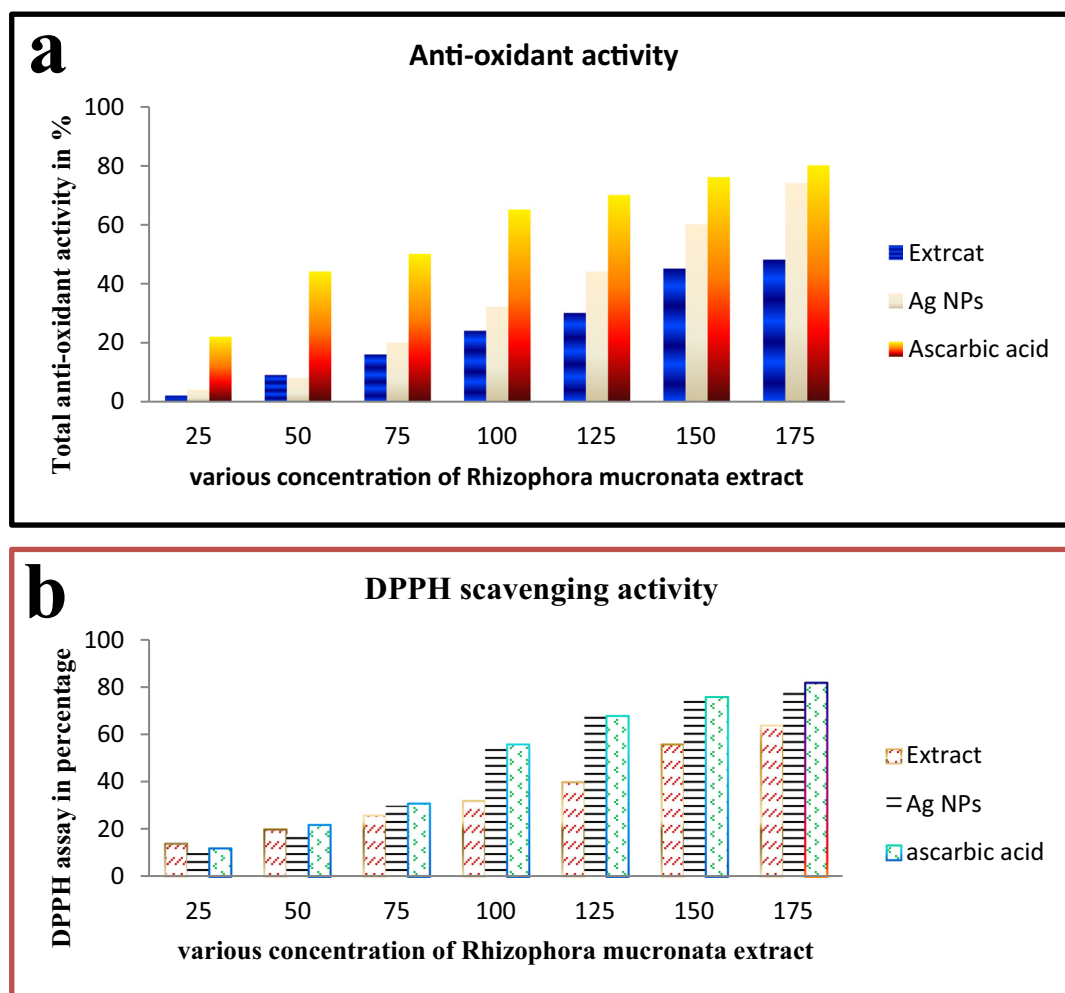


Fig. 3. Total anti-oxidant (a) and DPPH scavenging activity (b) of *Rhizophora mucronata* extract by invitro studies.

72%. When compared with extract 64%, it was high. Instead, it showed low activity compared with positive control 87%. All the activities were also exhibited at 200 µg/mL concentration and shown in Fig. 3b. Previously Aji Jovitha et al. (Abdi et al., 2019) reported that the marine *Rhizophora mucronata* plant mediated Ag NPs has higher radical scavenging activity than extract and it may influence by Ag NPs. Similarly, Abdi (Zhou et al., 2013) reported that the plant mediated Ag NPs exhibited more anti-oxidant activity and DPPH radical scavenging activity at lowest concentration. Supported evidence of Umashankari (Vijaya Sankar and Abideen, 2019) reported, highest content of phenolic and flavonoid rich sources of plant has excellent anti-oxidant activity and also various biological properties like anti-microbial, anti-cancer, larvicidal and etc.. Sometimes, the increased biological activity of Ag NPs was stimulated by selected plant due to the absorption of nutrients, hormones and other stress responding genes (Yang et al., 2020).

3.4. Characterization of Ag NPs

Synthesized Ag NPs surface plasmon resonance was indicated at the place of 415 nm, and it shown in Fig. 4a. The colored solution was changed to no color after addition of *Rhizophora mucronata* extract at 1 h. The greenish yellow color formation was indicated that the Ag was converted to Ag NPs in the presence of *Rhizophora mucronata* extract and it suggested with SPR vibrations. The result

was good agreement with (Uzma et al., 2020; Titkov et al., 2017) and the range between 410 and 440 is SPR of Ag NPs. In addition, intensity of XRD binding energy was suggest, the three major and two minor diffraction peaks at the position of 30.12, 39.30, 42.34, 51.04, and the respective planes were shown at 61.22 111, 200, 202, 221, 224 (Fig. 4b). The result was clearly revealed that the Ag + ion was transferred in the plant extract and produced the Ag NPs without any impurities. The supportive evidence of Mi theory was significantly correlated with our result (Mortazavi-Derazkola et al., 2020; Al-kawmani et al., 2020).

Further, the surface plasmon resonance of synthesized Ag NPs was shown with extremely agglomerated spherical shape morphology (Fig. 5) by SEM view (Titkov et al., 2017; Dinparvar et al., 2020).

3.5. Anti-cancer studies

3.5.1. Cell viability of Ag NPs

The cell viability was decreased continuously after treatment with Ag NPs at the concentration of 150 µg/mL. Mechanistically, the Ag interacts with nuclear membrane of cancer cells and induced more apoptosis. After apoptosis, the cell growth was decreased due to the depletion of nutrients and increased efficiency of Ag NPs in target sites (Ghosal et al., 2020). In result, if the Ag NPs was increased, the cell viability was decreased. The result proved, silver nanoparticle is a concentration dependent

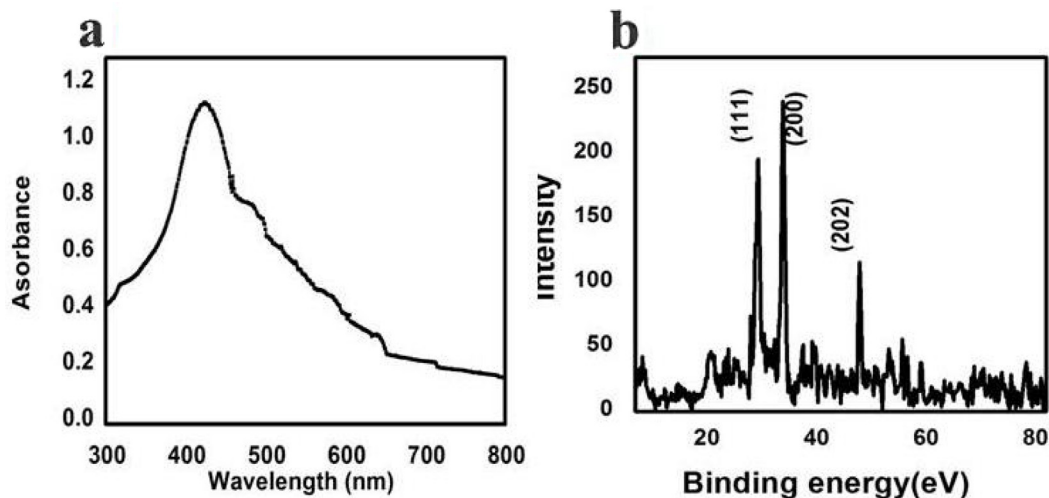


Fig. 4. UV-spectrometer (a) and XRD pattern reports of *Rhizophora mucronata* extract mediated Ag NPs.

anti-cancer agent against MCF-7 breast cancer cells. At 10 $\mu\text{g}/\text{mL}$ concentration of Ag NPs was started their inhibition role in viability, and it extended to 51% of cell death at 75 $\mu\text{g}/\text{mL}$ concentration. The complete deactivation of cancer cell survival rate was observed at the concentration of 150 $\mu\text{g}/\text{mL}$ (Fig. 6a). This concentration was very efficient compared with any other concentration. The deactivation was started in the death time of half and complete growth cell arrest was received at 150 $\mu\text{g}/\text{mL}$ concentration. Previously, the low concentration of biosynthesized Ag NPs was observed against cancer cells by Naveen Kumar et al. (2018). Also, reported that the biosynthesized Ag NPs has the ability to inactivate the cancer cells through growth cell arrest and mitochondrial damages. The viability was observed after addition of MTT solution, in this condition, the treated wells were shown with color changes due to the effect of formazan production. Based on the detected result of this study was indicated that the 150 $\mu\text{g}/\text{mL}$ concentration was fixed as IC_{50} concentration. The current result was more correlated to available biomolecules interacted with Ag NPs in mixture combination and enhances the inhibition role in MCF-7 lung cancer cells through apoptosis or necrosis. Compared with previous reports, the seaweed of *Sargassum wightii* is excellent source for synthesis of Ag NPs with enhances anti-cancer properties. In addition,

the 150 $\mu\text{g}/\text{mL}$ concentration against MCF-7 lung cancer was very lowest concentration compared to previous Ag NPs by biological route (Almalki and Khalifa, 2020; Uzma et al., 2020).

3.5.2. Phase contrast microscopy

Fig. 6b, c was suggested the death and live cells of treated and control wells. Before intracellular inhibition of Ag NPs against MCF-7 cell lines, the shrank and rough surface of MCF-7 cells was shown by phase contrast microscope after 24 h inhibition. Compared with control, the treated cells were shown irregular, detachment, rough and confused colonies (Fig. 6b). In addition, the treated wells containing solutions were low turbidity and confluence colonies were shown on cover slip after viewed by phase contrast microscope. The differentiation was identified easily by control and treated images due to the respective tightly clumped colonies and loosely arranged colonies of MCF-7 lung cancer. The initial morphological differentiation of phase contrast images were agreed by previous report of Venugopal et al. (Ramesh et al., 2018). Detection of intense damaged cells after treatment with the help of phase contrast microscope. (Ghosal et al., 2020). Similar result was also reported by Solairaj et al. (Mortazavi-Derazkola et al., 2020), and the resulted evidences were more useful to compare treatment effect of silver nanoparticle.

3.5.3. Fluorescence microscopic confirmation

After phase contrast microscope analysis, the confirmation of morphological damages in the Ag NPs treated Ag NPs were viewed by fluorescence microscope using two different fluorescence dyes named as AO/EB (Fig. 6e, d). The live and death cells differentiation was easily identified in AO/EB mediated fluorescence staining assay due to the light intensity observation (Al-kawmani et al., 2020). AO is a green dye having the ability to bind in inside of the cancer cells. Whereas, EB is another fluorescence dye having the binding nature of damaged cells (Saravanakumar et al., 2019). After treatment with biosynthesized Ag NPs of our study result was indicated that the Ag Nps was effectively inhibited the MCF-7 cells effectively. The damage cells were absorbed the EB dye and emitted red color fluorescence images in fluorescence microscope. Compared to control, the treated cells were shown with irregular morphology and more condensed colonies. More places were shown with orange color, indicating the more apoptosis was processed in inside of the cells. The usual shapes were completely modified due to the effect of Ag NPs, instead the regular and normal shapes were confirmed.

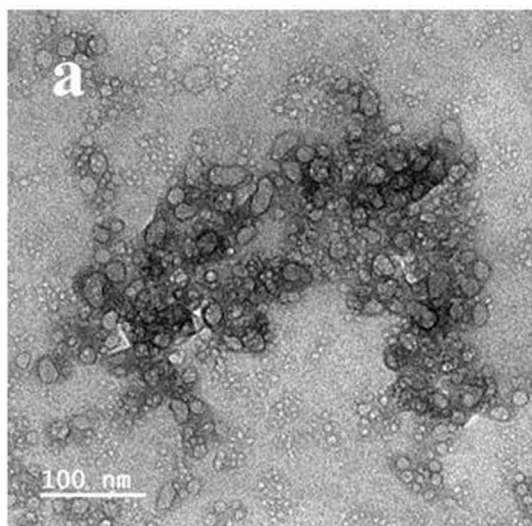


Fig. 5. Scanning electron microscope of *Rhizophora mucronata* extract mediated Ag NPs.

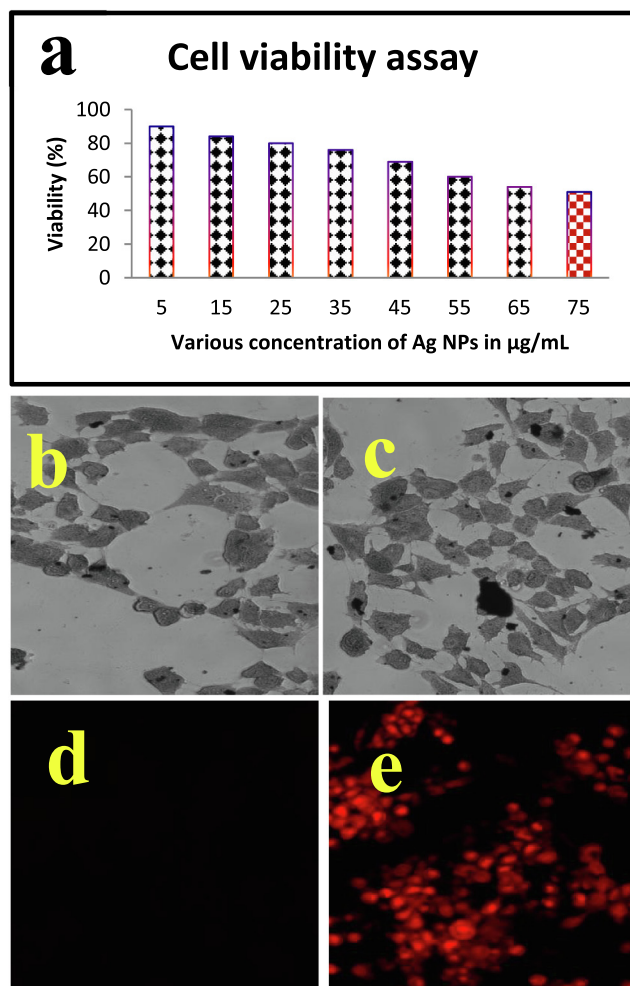


Fig. 6. Percentage of cell viability (a) and IC50 concentration of Ag NPs treated MCF-7 breast cells by phase contrast microscope (b, c) and live/dead cells differentiation (d, e) by fluorescence microscope.

This differentiation was indicated that the damages were appeared in the Ag NPs treated cells. After inhibition of growth cells, the Ag Nps will not allow the cells to grow next stage or cell cycle process due to the block the nutrient and responsible factors (Parthasarathy et al., 2020; Ramesh et al., 2018). More ever, Ag NPs stimulated the cancer cells to maintain in decline phase and it leads to complete death. Previously, Kumar et al. (Mortazavi-Derazkola et al., 2020); Vijaya Anand et al. (Kumar et al., 2018) reported that the Ag NPs induce the nucleus membrane and produce more condensed cells and it continuously failed to reproduce further. This statement was agreed by Khorrami et al. (Vijaya Anand et al., 2019), reported that the biosynthesized Ag NPs has increased anti-cancer properties.

3.5.4. Photocatalytic studies

The concentration of Rho B was gradually reduced after addition of Ag NPs in time dependent manner (Fig. 7a). As compared to all the tested concentration 15 mg/L seems more efficiency remove the dye as compared to remaining concentrations (5 and 10 mg/L).

After 150mins of solar light irradiation reduces the amount Rho B from 85.29 to 10.67% this was relatively higher than the degradation of percentage of CV. The percentage was CV showed insignificant reduction even after exposure to higher concentration of Ag₂O NPs (Fig. 7b). Only 34.04% of CV was reduced after 150mins of Ag₂O NPs exposure. The photocatalytic activity of Ag NPs syn-

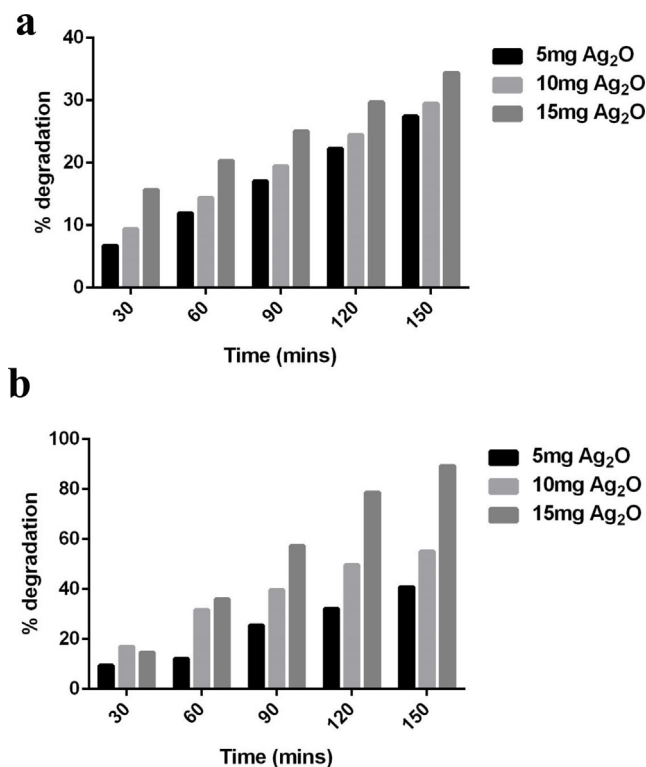


Fig. 7. Photocatalytic degradation of Rhodamine B dye (a) and crystal violet dye (b).

thesized via floral extract showed significant reduction of Rho B as compared to other studies. Around 40% of degradation was observed when Rho B was treated with Ag NPs prepared by thermal route (Rajivgandhi et al., 2019). On the other hand, *Alpinia nigra* fruit extract mediated Ag NPs produced 85.9% of Rho B degradation (Uzma et al., 2020), it was relatively equal to the catalytic efficiency of Ag NPs reported in this study. The present data implicated that the potential of Ag NPs towards the degradation of dye. When discussing with the molecular mechanics, faster degradation of Rho B was directly affected by free radicals generated during the light irradiation. Free radicles such as super oxide and hydroxyl radicles are directly related the dye degradation, however hydroxyl radicles are consider being the more powerful breaker. This result was also agreed by previous report of Khataee and Kasiri, (Tammina et al., 2017); Manal et al. (2021).

4. Conclusion

In this study, the marine mangrove plant *Rhizophora mucronata* extract has potential phenolic and flavonoid compounds. These phytochemical compounds were increased the anti-oxidant activity due to the marine environments including pH, temperature, NaCl, carbon and nitrogen sources. Further, the *Rhizophora mucronata* mediated Ag NPs enhances the anti-cancer effect against MCF-7 breast cancer cells at concentration dependent manner. The intracellular nucleus damages and ROS mediated damages on the nucleus, mitochondrial membrane and increased apoptosis was effectively detected by fluorescence microscopy analysis.

Declaration of Competing Interest

The authors declare that they have no known competing financial interests or personal relationships that could have appeared to influence the work reported in this paper.

Acknowledgement

All the authors gratefully acknowledge the National Natural Science Foundation of China (Project Approval Number: 41950410573) and Postdoctoral Science Foundation of China (Project Approval Number: 2019M663213) for financial support for this work. The authors extend their appreciation to the Researchers Supporting Project number (RSP-2021/70), King Saud University, Riyadh, Saudi Arabia. Wen-Jun Li was also supported by Introduction project of high-level talents in Xinjiang Uygur Autonomous Region.

References

Gomathi, A.C., Xavier Rajarathinam, S.R., Mohammed Sadiq, A., Rajeshkumar, S., 2020. Anticancer activity of silver nanoparticles synthesized using aqueous fruit shell extract of *Tamarindus indica* on MCF-7 human breast cancer cell line. *J. Drug Deliv. Sci. Technol.* 55, 101376.

Ramar, M., Manikandan, B., Marimuthu, P.N., Raman, T., Mahalingam, A., Subramanian, P., Karthick, S., Munusamy, A., 2015. Synthesis of silver nanoparticles using *Solanum trilobatum* fruits extract and its antibacterial, cytotoxic activity against human breast cancer cell line MCF 7. *Spectrochim. Acta A Mol. Biomol. Spectrosc.* 140, 223–228.

Almalki, M.A., Khalifa, A.Y.Z., 2020. Silver nanoparticles synthesis from *Bacillus* sp KFU36 and its anticancer effect in breast cancer MCF-7 cells via induction of apoptotic mechanism. *J. Photochem. Photobiol. B: Biolog.* 204, 111786.

Uzma, M., Sunayana, N., Raghavendra, V.B., Madhu, C.S., Shanmuganathan, R., Brindhadevi, K., 2020. Biogenic synthesis of gold nanoparticles using *Commiphora wightii* and their cytotoxic effects on breast cancer cell line (MCF-7). *Process Biochem.* 92, 269–276.

Titkov, A.I., Bulina, N.V., Ulihin, A.S., Shundrina, I.K., Karpova, E.V., Gerasimov, E.Y., Yukhin, Y.M., Lyakhov, N.Z., 2017. *N*-Lauroylsarcosine capped silver nanoparticle based inks for flexible electronics. *J. Mater. Sci.: Mater. Electron.* 28, 2029–2036.

Dinparvar, S., Bagirova, M., Allahverdiyev, A.M., Abamor, E.S., Safarov, T., et al., 2020. A nanotechnology-based new approach in the treatment of breast cancer: Biosynthesized silver nanoparticles using *Cuminum cyminum* L. seed extract. *J. Photochem. Photobiol. B* 208, 111902.

Ghosal, K., Ghosh, S., Ghosh, D., Sarkar, K., 2020. Natural polysaccharide derived carbon dot based in situ facile green synthesis of silver nanoparticles: Synergistic effect on breast cancer. *Int. J. Biol. Macromol.* 20, 34074–34075.

Jiang, L., Lu, X., Zheng, X., 2014. Copper/silver nanoparticle incorporated graphene films prepared by a low-temperature solution method for transparent conductive electrodes. *J. Mater. Sci.: Mater. Electron.* 25 (1), 174–180.

Mortazavi-Derazkola, S., Ebrahimzadeh, M.A., Hamid Reza Goli, O.A., Rafiei, A., Kardan, M., 2020. Facile green synthesis and characterization of *Crataegus microphylla* extract-capped silver nanoparticles (CME@Ag-NPs) and its potential antibacterial and anticancer activities against AGS and MCF-7 human cancer cells. *J. Alloy. Compd.* 820, 153186.

Al-kawmani, A.A., Alanazi, K.M., Farah, M.A., Ali, M.A., Hailan, W.A.Q., Al-Hemaid, F. M.A., 2020. Apoptosis-inducing potential of biosynthesized silver nanoparticles in breast cancer cells. *J. King Saud University – Sci.* 32 (4), 2480–2488.

Solairaj, D., Rameshthangam, P., Arunachalam, G., 2017. Anticancer activity of silver and copper embedded chitin nanocomposites against human breast cancer (MCF-7) cells. *Int. J. Biol. Macromol.* 105, 608–619.

Khorrani, S., Zarepour, A., Zarrabi, A., 2019. Green synthesis of silver nanoparticles at low temperature in a fast pace with unique DPPH radical scavenging and selective cytotoxicity against MCF-7 and BT-20 tumor cell lines. *Biotechnol. Rep.* 24, e00393. <https://doi.org/10.1016/j.btre.2019.e00393>.

Majeed, S., Binti Aripin, F.H., Binti Shoe, N.S., Danish, M., Mohamad Ibrahim, M.N., et al., 2019. Bioengineered silver nanoparticles capped with bovine serum albumin and its anticancer and apoptotic activity against breast, bone and intestinal colon cancer cell lines. *Mater. Sci. Eng. C* 102, 254–263.

Ramachandran, G., Rajivgandhi, G.N., Murugan, S., Alharbi, N.S., Kadaikunnan, S., Khaled, J.M., Almana, T.N., Manoharan, N., Li, W.-J., 2020. Anti-carbapenamase activity of *Camellia japonica* essential oil against isolated carbapenem resistant *Klebsiella pneumoniae* (MN396685). *Saudi J. Biolog. Sci.* 27 (9), 2269–2279.

Rajivgandhi, G.N., Ramachandran, G., Maruthupandy, M., Manoharan, N., Alharbi, N. S., Kadaikunnan, S., Khaled, J.M., Almana, T.N., Li, W.-J., 2020. Anti-oxidant, anti-bacterial and antibiofilm activity of biosynthesized silver nanoparticles using *Gracilaria corticata* against biofilm producing *K. pneumoniae*. *Colloids Surf. A: Physicochem. Eng. Aspects* 600, 124830. <https://doi.org/10.1016/j.colsurfa.2020.124830>.

Rajivgandhi, G.N., Maruthupandy, M., Li, J.L., Dong, L., Alharbi, N.S., et al. 2020. Photocatalytic reduction and antibacterial activity of biosynthesized silver nanoparticles against multi drug resistant *Staphylococcus saprophyticus* (MN310601). *Mater. Sci. Eng. C* 114, 111024.

Ramesh, A.V., Dharmasoth Rama Devi, Ganga Rao Battu, Basavaiah K. 2018. A Facile plant mediated synthesis of silver nanoparticles using an aqueous leaf extract of *Ficus hispida* Linn. f. for catalytic, antioxidant and antibacterial applications South Afr. J. Chem. Eng. 26, 25–34.

Saravanakumar, K., Chelliah, R., MubarakAli, D., Oh, D.H., Kathiresan, K., Wang, M.H., 2019. Unveiling the potentials of biocompatible silver nanoparticles on human lung carcinoma MCF-7 cells and *Helicobacter pylori*. *Sci Rep.* 9, 5787.

Kumar, S., Kang, T.W., Lee, S.J., Yuldashev, S., Taneja, S., Banyal, S., Singhal, M., Ghodake, G., Jeon, H.C., Kim, D.Y., Choubey, R.K., 2019. Correlation of antibacterial and time resolved photoluminescence studies using bio-reduced silver nanoparticles conjugated with fluorescent quantum dots as a biomarker. *J. Mater. Sci.: Mater. Electron.* 30 (7), 6977–6983.

Venugopal, K., Ahmad, H., Manikandan, E., Thanigai Arul, K., Kavitha, K., Moodleyf, M.K., Rajagopal, K., Balabhaskar, R., Bhaskarh, M., 2017. The impact of anticancer activity upon Beta vulgaris extract mediated biosynthesized silver nanoparticles (ag-NPs) against human breast (MCF-7), lung (MCF-7) and pharynx (Hep-2) cancer cell lines. *J. Photochem. Photobiol. B: Biol.* 173, 99–107.

Naveen Kumar, S., Rajivgandhi, G., Manoharan, N., 2018. Cytotoxicity effect of marine Sponge Alkaloid, Fascaplysin on HepG2 Hepatocellular carcinoma cell. *Fron. Lab. Med.* 2, 41–48.

Tammina, S.K., Mandal, B.K., Ranjan, S., Dasgupta, N., 2017. Cytotoxicity study of *Piper nigrum* seed mediated synthesized SnO₂ nanoparticles towards colorectal (HCT116) and lung cancer (MCF-7) cell lines. *J. Photochem. Photobiol. B: Biol.* 166, 158–168.

Khataee, A.R., Kasiri, M.B., 2010. Photocatalytic degradation of organic dyes in the presence of nanostructured titanium dioxide: Influence of the chemical structure of dyes. *J. Mol. Catal. A: Chem.* 328 (1–2), 8–26.

Yang, X., Rajivgandhi, G.N., Ramachandran, G., Alharbi, N.S., Kadaikunnan, S., et al., 2020. Preparative HPLC fraction of *Hibiscus rosa-sinensis* essential oil against biofilm forming *Klebsiella pneumoniae*. *Saudi J. Biol. Sci.* <https://doi.org/10.1016/j.sjbs.2020.07.008>.

Aji Jovitha, A.T., Deivasigamani, B., 2020. Biosynthesis and characterization of silver nanoparticles from mangrove bark – *Rhizophora mucronata* extract. *Asian J. Pharm. Clin. Res.* 13, 1–4.

Abdi, V., Sourinej, I., Yousefzadi, M., Ghasemi, Z., 2019. Biosynthesis of silver nanoparticles from the mangrove *rhizophora mucronata*: its characterization and antibacterial potential. *Iran. J. Sci. Technol. Trans. Sci.*, 1–10

Zhou, Y., Gao, L., An, G., Yang, C., Zhao, X., 2013. Facile method to synthesize polystyrene/silver composite nanoparticles with core-shell structures. *J. Mater. Sci.: Mater. Electron.* 24 (6), 2156–2160.

Vijaya Sankar, M., Abideen, S., 2019. Biosynthesis of silver nanoparticles using *Rhizophora mucronata* and *Cerriops decandra* and their antagonistic activity on gut cellulolytic bacteria. *Int. J. Pharmaceut. Biolog. Archiv.* 10, 138–145.

Parthasarathy, A., Vijayakumar, S., Malaikozhundan, B., Thangaraj, M.P., Ekambaram, P., Murugan, T., Velusamy, P., Anbu, P., Vaseeharan, B., 2020. Chitosan-coated silver nanoparticles promoted antibacterial, antibiofilm, wound-healing of murine macrophages and antiproliferation of human breast cancer MCF 7 cells. *Polym. Test.* 90, 106675. <https://doi.org/10.1016/j.polymertesting.2020.106675>.

Mortazavi-Derazkola, S., Ebrahimzadeh, M.A., Amiri, O., Goli, H.R., Rafiei, A., Kardan, M., Salavati-Niasari, M., 2020. Facile green synthesis and characterization of *Crataegus microphylla* extract-capped silver nanoparticles (CME@Ag-NPs) and its potential antibacterial and anticancer activities against AGS and MCF-7 human cancer cells. *J. Alloy. Compd.* 820, 153186. <https://doi.org/10.1016/j.jallcom.2019.153186>.

Kumar, P., Yuvakkumar, R., Vijayakumar, S., Vaseeharan, B., 2018. Cytotoxicity of phloroglucinol engineered silver (Ag) nanoparticles against MCF-7 breast cancer cell lines. *Mater. Chem. Phys.* 220, 402–408.

Vijaya Anand, M.A., Vinayagam, R., Vijayakumar, S., Balupillai, A., Herbert, F.J., Kumar, S., 2019. Green synthesis, characterization and antibacterial activity of silver nanoparticles by *Malus domestica* and its cytotoxic effect on (MCF-7) cell line. *Microb. Pathog.* 135, 103609.

Rajivgandhi, G., Maruthupandy, M., Quero, F., Li, W.J., 2019. Graphene/nickel oxide nanocomposites against isolated ESBL producing bacteria and MCF-7 cancer cells. *Mater. Sci. Eng. C* 102, 829–843.

Uzma, M., Sunayana, N., Raghavendra, V.B., Madhu, C.S., Shanmuganathan, R., et al., 2020. Biogenic synthesis of gold nanoparticles using *Commiphora wightii* and their cytotoxic effects on breast cancer cell line (MCF-7). *Process Biochem.* 92, 269–276.

Manal, A.A., Awatif, A.H., Khalid, M.O., Batool, A., ina, S., Amnah, A., Wadha, A., Rasha Mohammed, T., Rasha, R., Maha, T., Najla, A.M., Taghrid, S.A. 2021. Biogenic synthesis of silver nanoparticles using *Trigonella foenum-graecum* seed extract: characterization, photocatalytic and antibacterial activities, *Sens. Actuat. A: Phys.* 323, 112670.